Title

A subtype of cerebrovascular pericytes is associated with blood-brain barrier disruption that develops during normal aging and simian immunodeficiency virus infection

Authors

Bohannon, Diana G
Okhravi, Hamid R
Kim, Jayoung
et al.

Publication Date

2020-12-01

DOI

10.1016/j.neurobiolaging.2020.08.006

Peer reviewed

HHS Public Access

Author manuscript

Neurobiol Aging. Author manuscript; available in PMC 2021 December 01.

Published in final edited form as:

Neurobiol Aging. 2020 December ; 96: 128–136. doi:10.1016/j.neurobiolaging.2020.08.006.

A subtype of cerebrovascular pericytes is associated with blood-brain barrier disruption that develops during normal aging and simian immunodeficiency virus infection

Diana G. Bohannon[a], **Hamid R. Okhravi**[b], **Jayoung Kim**[c], **Marcelo J. Kuroda**[d], **Elizabeth S. Didier**[d], **Woong-Ki Kim**[a,*]

[a]Department of Microbiology and Molecular Cell Biology, Eastern Virginia Medical School, Norfolk, Virginia, United States

[b]Glennan Center for Geriatrics and Gerontology, Eastern Virginia Medical School, Norfolk, Virginia, United States

[c]Cedars-Sinai Medical Center, University of California, Los Angeles, Los Angeles, California, United States

[d]Center for Immunology and Infectious Diseases, University of California, Davis, Davis, California, United States

Abstract

Lax phenotypic characterization of these morphologically distinct pericytes has delayed our understanding of their role in neurological disorders. We herein establish markers which uniquely distinguish different subpopulations of human brain microvascular pericytes and characterize them independently from cerebrovascular smooth muscle cells. Furthermore, we begin to elucidate the roles of these subsets in blood-brain barrier (BBB) breakdown by studying natural aging and simian immunodeficiency virus (SIV) infection in rhesus macaques. We demonstrate that the main type-1 pericyte subpopulation in the brain of young uninfected adults is positive for platelet-derived growth factor receptor-β (PDGFRB) and negative for α-smooth muscle actin (SMA) and myosin heavy chain 11 (MYH11), while PDGFRB+/SMA+/MYH11− (type-2) pericytes are found more frequently in older adults and are associated with SIV infection and progression.

*Corresponding author at: Department of Microbiology and Molecular Cell Biology, Eastern Virginia Medical School, 700 W. Olney Road, Lewis Hall 3174, Norfolk, VA, 23501, USA. Tel.: 757-446-5639. kimw@evms.edu (W.-K. Kim).

Authorship statement: D.G.B. carried out the experiments, analyzed data and drafted the article; H.R.O. participated in scientific discussion and edited the article; J.K. participated in scientific discussion and edited the article; M.J.K. co-directed the animal experiments, participated in scientific discussion and edited the article; E.S.D. helped in procuring the macaque brain tissue, participated in scientific discussion and edited the article; W.-K.K. conceptualized, designed and coordinated the study and edited the final version of the article. All authors read and approved the final version.

Disclosure statement

The authors declare that there is no conflict of interest.

All authors verify that the data contained in the manuscript being submitted have not been previously published, have not been submitted elsewhere and will not be submitted elsewhere while under consideration at Neurobiology of Aging.

We also verify that appropriate approval and procedures were used concerning human subjects and animals.

Interestingly, we find a strong positive correlation between the degree of BBB breakdown and the percentage of type-2 pericytes regardless of age or SIV status. Taken together, our findings suggest that type-2 pericytes may be a cellular biomarker related to BBB disruption independent of disease status.

Keywords

Aging; Brain; HIV; Pericyte; Smooth muscle cell

1. Introduction

The blood-brain barrier (BBB) is responsible for maintaining the tightly controlled brain environment which neurons and other support cells require to function optimally. Consisting of endothelial cells held together by tight junction proteins (TJPs), pericytes surrounded by the basement membrane, and astrocytic endfeet, the BBB is a complex network of cells that collaborate to form a selectively permeable membrane allowing necessary nutrients into the brain and keeping blood proteins and other toxins out (Persidsky et al., 2006; Zhao et al., 2015). Pericytes play multiple roles within the BBB, acting not only as a secondary barrier beyond endothelial cells, but also as environmental sensors and regulators (Armulik et al., 2010; Krueger and Bechmann, 2010). During angiogenesis in the brain, pericytes are essential for recruiting astrocytes and initiating the production of basement membrane proteins which solidify the BBB (Balabanov and Dore-Duffy, 1998; Jeon et al., 1996; Stratman et al., 2010). Further, evidence suggests that they are involved in the production of netrin-1 which is essential for the sonic hedgehog pathway-induced production of TJPs (Bohannon et al., 2019; Podjaski et al., 2015). Pericytes are also highly sensitive to changes in the BBB microenvironment allowing them to adjust regulatory mechanisms to maintain BBB homeostasis under mild pathological conditions (Armulik et al., 2010; Sweeney et al., 2016).

In incidences when the pathological strain becomes too great, however, pericyte loss has been noted and has been shown to have a significant detrimental impact on BBB heath. A loss of pericytes from the BBB has been shown to significantly increase the amount of blood extravasating into the brain parenchyma (Armulik et al., 2010; Nakazato et al., 2017; Sengillo et al., 2013; Villasenor et al., 2017). In addition, studies in cell cultures and transgenic mouse models have shown that a loss of pericytes or pericyte function results in a reduction in TJPs, an increase in cellular migration across the BBB, and a loss of basement membrane proteins (Armulik et al., 2010; Wang et al., 2012).

While these mouse models of complete pericyte deficiency are extreme and not known to occur in humans, morphological abnormalities of human pericytes in many neuropathologies are prevalent throughout literature. Abnormal brain pericyte morphology has been shown in diseases from human immunodeficiency virus (HIV) to neutrophilic dermatosis to natural aging (Castejon, 2011; Lauridsen et al., 2017; Peters and Sethares, 2012). These morphologically abnormal pericytes often appear hypertrophied, contain dark granules and are found in regions of the BBB that have undergone basement membrane remodeling

(Bohannon et al., 2019; Lauridsen et al., 2017; Peters and Sethares, 2012). Currently, however, there is no clear consensus about the nature or function of these morphologically distinct pericytes. We sought to establish markers which uniquely distinguish different subpopulations of the primate CNS microvasculature and began to assess their impact on BBB functionality.

2. Materials and methods

2.1. Human brain tissue

Formalin-fixed paraffin-embedded (FFPE) human brain tissues containing Brodmann area 10 (BA10) were obtained from the NIH NeuroBioBank, sectioned and mounted as 5-μm thick sections on glass slides. A total of three young adult (20–35 years) and three aged adult (Fuller et al., 2004) unaffected control patients were used in this study (Table 1a). The study was determined to be “Not Human Subjects Research” by the Institutional Review Board of Eastern Virginia Medical School (IRB # 18-04-NH-0103).

2.2. Animal cohorts

This study was performed using archived FFPE tissue blocks of the frontal cortex from 40 rhesus macaques (*Macaca mulatta*) that were housed and euthanized at the Tulane National Primate Research Center (TNPRC) in accordance with Tulane University’s IACUC regulations and TNPRC endpoint policies. Both males and females were used for uninfected juveniles (n = 10, age: 0–3.99 year), uninfected young adults (n = 10, age: 4–11 years), and uninfected aging adults (n= 10, age: 17–30 years) macaques (Table 1b). Five uninfected young adult males were used when comparing simian immunodeficiency virus (SIV)-infected macaques without encephalitis (SIVnoE) (n = 5, age: 4–11 years), and SIV-infected with encephalitis (SIVE) (n = 5, age: 4–11 years), all of whom were male (Table 1b). SIV infection was achieved through intravenous injection of SIVmac251 and SIVE animals were CD8 depleted to achieve rapid progression of encephalitis. SIVE status was determined by the presence of SIV Gag proteins in the brain, accumulation of macrophages, and the presence of multinucleated giant cells.

2.3. Immunofluorescence microscopy

Immunofluorescence (IF) microscopy was performed using the antibodies listed in Table 2 with validation using negative and positive controls. Briefly, sections underwent deparaffinization by overnight incubation at 60ºC prior to serial xylene and rehydrating ethanol baths. Antigen retrieval pre-treatment was performed with citrate-based antigen unmasking solution (Vector Laboratories) in the microwave for 20 min. After cooling in solution for 20 min, slides were dipped in distilled water and washed in phosphate-buffered saline (PBS) with 0.2% fish skin gelatin (FSG) (PBS/FSG). Sections were then permeabilized with PBS/FSG containing 0.1% Triton X-100 for 1 h before a pair of PBS/FSG washes. Sections were then blocked in 5% goat serum for 30 min to 1 h before immediate application of the primary antibody diluted in PBS/FSG as specified in Table 2 for 1 h. After a series of PBS/FSG baths the desired secondary antibody was applied for 1 h and another round of PBS/FSG baths were performed. Subsequent primary and secondary antibodies were added as described above to achieve two- to five-color IF staining. After the

final secondary antibody, a set of PBS/FSG washes was performed followed by a dip in distilled water before the sections were soaked in 10mM $CuSO_4$ for 45 min. The slides were then returned to distilled water before being mounted using a glass coverslip and Aqua-Mount mounting medium (Thermo Scientific).

Fluorescent microscopy images were taken on a Zeiss Axio Observer .Z1 fluorescent microscope with a 40x oil emersion objective. Zeiss AxioVision 4.9.1 edition was used to capture and merge images. Confocal images were taken with a Zeiss 880 Laser scanning confocal microscope with a 63x or 100x oil emersion objective. ZenBlack and ZenBlue programs were used to capture and merge images.

2.4. Quantitative analysis

Quantitative analysis was performed using ImageJ. The inner (luminal) diameter was measured as the shortest distance between the inside edges across each vessel through the center point of the lumen using the ImageJ linear measure tool. The percentage of pericytes that are type-2 pericytes was determined by observing 100 pericytes in random fields for each animal and counting the numbers of type-1 and type-2 pericytes present in each. The percentage of vessels with fibrinogen extravasation was determined as shown previously by measuring the pixel intensity of glucose transporter 1 (GLUT1) and fibrinogen using dual overlay histograms to determine whether fibrinogen exists outside of the GLUT1+ vessel peaks for each of 25 microvessels (<10 um diameter) per animal (9, 18). Mean pixel intensity (MPI) of claudin 5 was determined by selecting an area encompassing pericytes and endothelial cells in ImageJ and measuring the MPI of claudin 5 using a pre-established threshold limit to eliminate background evenly for all images. No lesion-associated vessels in SIV infected animals were used in this study.

2.5. Statistical analysis

GraphPad Prism 7.2 was used to produce graphs and perform statistical analysis. Statistical tests performed are included in each figure legend and significant p-values are represented on the graph by asterisks. Linear regression r^2 values and p values are on each applicable graph. * denotes $p < 0.05$, ** denotes $p < 0.01$, *** denotes $p < 0.001$, **** denotes $p < 0.0001$.

3. Results

3.1. Distinct SMA-positive cells observed in microvasculature of aging human brain

The precise definition of pericytes has been a subject of debate in the field for many years. A vast multitude of human pericyte markers are used such as CD13, CD146, desmin, nestin, NG2, platelet-derived growth factor receptor β (PDGFRB), and α-smooth muscle actin (SMA), but none of these specifically distinguish pericytes from endothelial cells or smooth muscle cells (SMCs) (Attwell et al., 2016; Guillemin and Brew, 2004). In particular, the presence of SMA in microvascular pericytes has been widely debated (Alarcon-Martinez et al., 2018; Attwell et al., 2016; Grant et al., 2019; Guillemin and Brew, 2004; Hartmann et al., 2015; Herman and D'Amore, 1985). Traditionally, it was thought that all perivascular cells with SMA were SMCs, but many report SMA+ cells around vessels of less than 10 μm

in luminal diameter, a microvascular sub-niche which is considered to be surrounded by pericytes not SMCs (Alarcon-Martinez et al., 2018; Attwell et al., 2016; Hartmann et al., 2015). Many explanations for this discrepancy have been suggested, but one possible explanation is that these SMA-positive and -negative vascular cells represent two distinct subpopulations of pericytes. When we examined both the changes in BBB integrity and morphological changes in the BBB in the BA10 of aging humans, we found two morphologically distinct subpopulations of PDGFRB+ cells around vessels less than 10 μm in luminal diameter. Interestingly, while young adults displayed primarily PDGFRB+SMA− pericytes in the brain, aging adults showed a significantly higher percentage of PDGFRB+ hypertrophic microvascular cells that express SMA (Fig. 1). Considering that BBB breakdown occurs during natural human aging, we sought to investigate if these PDGFRB +SMA+ microvascular cells represent a distinct subtype of pericytes that might play a role in BBB disruption (Farrall and Wardlaw, 2009; Montagne et al., 2015). The paucity of autopsy brain tissue from uninfected normal healthy subjects prompted us to use nonhuman primates (NHP) as an animal model of human aging and brain aging. The use of NHP in all subsequent experiments also enabled us to closely investigate age-dependent changes in pericytes and BBB over the course of lifespan similar to that of humans.

3.2. Type-2 pericytes are SMA-positive, but -negative for other smooth muscle cell markers

While pericytes have been classically defined as PDGFRB-positive, SMA-negative cells, and SMCs have been defined as double-positive cells, modern literature suggests that differentiating between these two cell types is much more complicated and that a distinct division is often hard to achieve (Boado and Pardridge, 1994; Dore-Duffy and Cleary, 2011; Skalli et al., 1989; Verbeek et al., 1994). Both pericytes containing SMA and subgroups of hybrid SMC-pericyte cells have complicated the task of differentiating pericytes and SMCs in vivo (Crisan et al., 2009; Hartmann et al., 2015; Skalli et al., 1989). It is, therefore, important not only to identify markers that specifically distinguish PDGFRB+/SMA− type-1 pericytes (PC1) and PDGFRB+/SMA+ type-2 pericytes (PC2), but also to firmly demonstrate that neither of these cell subtypes are SMCs and establish markers which can be used to differentiate them in vivo. A smooth muscle myosin (myosin-11, MYH11) belonging to the myosin heavy chain family is exclusively expressed in SMCs and a recent RNA-seq study comparing the transcriptomic profile of SMCs and pericytes isolated from the rat brain demonstrated that myosin-11 mRNA was highly specific for brain SMCs (Chasseigneaux et al., 2018; Kumar et al., 2017). Therefore, we sought to investigate if this specifically marks brain SMCs in rhesus macaques. Triple IF staining demonstrated that PC1 were PDGFRB+/SMA−/MYH11−, while PC2 were PDGFRB+/SMA+/MYH11−, and SMCs were PDGFRB+/SMA+/MYH11+ (Fig. 2a-c). PC1 and PC2 are often found on microvessels of equivalent branching order, indicating that they coexist on CNS vessels of the same type, size, and location (Fig. 2d). Historically, the size of the vessel with which a perivascular cell is associated has been a criterion used to differentiate SMCs and pericytes with pericytes being associated with vessels smaller than 10 μm in luminal diameter in humans and NHP and SMCs being associated with larger vessels (arteries and arterioles) (Attwell et al., 2016; Grant et al., 2019; Hartmann et al., 2015). Vessels associated with PC2 have a similar luminal diameter to vessels associated with PC1 that is less than 10 μm, while

vessels associated with SMCs have significantly larger average luminal diameter (Fig. 2e). A recent study identified mural cells, with a mixed phenotype of SMCs and pericytes, which are located at the junction between the arterioles and the precapillary arterioles (Grant et al., 2019; Hartmann et al., 2015). These “smooth muscle-pericyte hybrid cells” do not fit the characterization of PC2 that include its coverage of vessels as small as 3 μm in luminal diameter (data not shown). We, therefore, believe that PC2 are a subset of classical microvascular pericytes and not SMC-pericyte hybrid cells (Grant et al., 2019; Hartmann et al., 2015).

3.3. Percentage of type-2 pericytes increases with age and BBB breakdown

Having established reliable markers to differentiate PC1, PC2, and SMCs, we sought to investigate whether the proportions of brain PC2 are increased with aging in rhesus macaques in support of our findings in the human pre-frontal cortex. For this, we looked at the percentage of PC2 among total PDGFRB+ microvascular pericytes (%PC2) in the frontal cortex of juvenile, young adult and aging rhesus macaques. We found a significant positive correlation between age and %PC2, indicating the %PC2 increases with age (Fig. 3a). Similarly, we found that the percentage of vessels demonstrating fibrinogen extravasation, an indicator of BBB breakdown, showed a strong positive correlation to age (Fig. 3b). The percentage of CNS microvessels with fibrinogen extravasation was positively correlated with the %PC2 in rhesus macaques, suggesting that PC2 may contribute to BBB breakdown natural aging (Fig. 3c).

3.4. Type-2 pericytes are less BBB supportive than type-1 pericytes

The relationship between PC2 and BBB breakdown motivated us to examine levels of fibrinogen extravasation between vessels with PC1 and PC2 coverage (Fig. 4a). While less than 20% of the microvessels associated with PC1 showed fibrinogen extravasation, more than 80% of the microvessels associated with PC2s showed fibrinogen extravasation, and no significant differences were found in the proportions of microvessels associate with PC2 demonstrating fibrinogen extravasation across age groups (Fig. 4b,c). This suggests that an increase in fibrinogen extravasation may be dependent upon an increased number of PC2 rather than an increased likelihood for a PC2-associated vessel to display fibrinogen extravasation. One possible reason for this increase in fibrinogen extravasation in vessels with PC2 coverage is a reduction in signaling cascades necessary for the production of TJPs. In fact, claudin 5 immunoreactivity was decreased in PC2 and their associated vessels compared to PC1s, but maintained consistent expression amongst PC2 and associated vessels of different age groups (Fig. 4d-f). Collectively, this suggests that PC2 are less BBB supportive than PC1 and that the changes in BBB stability seen with aging are likely associated with the increased %PC2 in aged individuals.

3.5. Increase in %PC2 also occurs after SIV infection as a general response to BBB breakdown

To determine whether an increased %PC2 is specific to the neuropathological model of aging, we studied the %PC2 in uninfected (UI) and SIV-infected young adult rhesus macaques with or without SIVE (Table 1b), an NHP model of HIV infection. The %PC2 was significantly higher in the SIVE group than in each of the 2 other young adult groups

(UI and SIVnoE). SIVnoE animals had a significantly higher %PC2 than uninfected animals (Fig. 5a). Similarly, fibrinogen extravasation was significantly increased in the SIVE group compared to both UI and SIVnoE groups, and neither the percentage of vessels with fibrinogen extravasation nor MPI of claudin 5 changed within PC2 by group (Fig. 5b-d). The significant positive correlation between the percentage of vessels with fibrinogen extravasation and the %PC2 persisted even when the aging cohorts and SIV cohorts are combined indicating that the correlation between fibrinogen extravasation and %PC2 is not an artifact of aging or an effect of SIV infection, but a more global indicator of BBB disruption (Fig. 5e).

4. Discussion

The presence of morphologically abnormal pericytes in association with aging has been described throughout literature, but these cells have never been independently classified as a subset of classical pericytes, nor have appropriate markers been assigned to identify their presence in vivo. Previously, we showed that hypertrophied pericytes were strongly localized in areas with fibrinogen extravasation indicative of BBB disruption (Bohannon et al., 2019). In the current study, by determining markers specific to PC1, PC2, and SMCs, we have established a mode by which these cells can be studied and their impact on BBB support or breakdown more thoroughly understood. We have sought to investigate how the presence of PC2 is associated with natural aging and CNS infection using SIV as a model. We herein show that while %PC2 is positively correlated to both age and SIV infection, %PC2 is strongly correlated to the degree of BBB breakdown independently of age or disease. Since the BBB is known to break down in both natural aging and SIV infection, we propose that the increase in %PC2 is directly tied to the increase in fibrinogen extravasation instead of being an artifact of any specific model of disease. This could be due to the decreased production of TJPs seen in PC2-associated vessels or due to other changes in BBB regulatory pathways which we have not yet studied. Ultimately, we speculate that PC2 have an intrinsic dysregulation of BBB-supporting pathways compared to PC1 and they play a primordial role in the development of age-related neurocognitive decline and cognitive impairment in patients with Alzheimer’s disease and HIV-associated neurocognitive disorders.

While a wide variety of pericyte markers are commercially available, their expression status in PC1 and PC2 cells is not yet known. Here, we demonstrate that PDGFRB, SMA, and MYH11 provide a successful combination for positively identifying these subsets in vivo. While other markers may also prove useful, the practicality of other commercially available pericyte markers may be limited. For example, desmin is a nuclear stain which increases the likelihood of a pericyte being misidentified at lower resolution or magnification levels. Similarly, while CD13 is a very popular pericyte marker, its presence has been shown in endothelial cells and therefore does not resolutely identify pericytes or their subsets (Bhagwat et al., 2001). In addition, many pericyte markers have been shown to occur in “High”, “Medium”, or “Low” levels on various pericyte, endothelial, and SMC subsets, which requires a certain amount of subjectivity when determining the identity of a cell in vitro or in vivo (Kumar et al., 2017). The use of PDGFRB, SMA, and MYH11 in concert provides a set of whole-cell, pericyte-specific markers, which are non-subjective and

distinguish PC1 and PC2 from SMCs. While it is unclear where PC2 originate from, our results suggest that PC2 are pericytic rather than of SMCs. PC2 become more abundant under pathological conditions, and they may play a distinct role in BBB maintenance and breakdown, making them an important cell population to study in relation to neurovascular health and disease.

The present study may help reveal functional differences between PC1 and PC2 in neurovascular health and disease. While we were able to show that both PC1 and PC2 are present of cerebral microvasculature of the same branching order, PC2 express α-SMA, a contractile actin isoform in found in SMCs around larger vessels. The presence of SMA could potentially indicate pericytes with contractile activity, which, in vessels smaller than 10 um in luminal diameter, may lead to the increased fibrinogen extravasation observed when ischemia occurs (Costa et al., 2018; Fernandez-Klett and Priller, 2015). Further research is warranted to determine the extent to which PC2 affect the microvasculature and to what degree they functionally differs from PC1. Establishing a system to differentiate them is the first fundamental step in achieving this goal.

This work provide a novel conceptual platform to explain functional differences between PC1 and PC2 in human and rhesus macaque tissues. Due to the strong positive correlation between %PC2 and BBB breakdown measured by fibrinogen extravasation, we propose that %PC2 can be used as an in situ biomarker for BBB breakdown. We speculate that PC1 are becoming PC2 under pathogenic conditions and intend to investigate whether this transition releases biomarkers which could be peripherally identified. Markers which are released during this shift and are measurable in the cerebrospinal fluid or serum could act as clinically relevant biomarkers to measure BBB breakdown. Further investigation of this unique subset of pericytes which are found in areas of BBB breakdown could lead to a deeper understanding of how BBB disruption occurs and provide new targets for diagnosis or treatment of patients suffering from neurodegenerative disorders.

5. Conclusions

We herein demonstrate the presence of PC2, a distinct subset of pericytes, which are hypertrophic and are almost exclusively found in areas containing fenestrated microvessels. PC2 are associated with vessels with less claudin-5 coverage and more fibrinogen extravasation than PC1 in both aging and SIV infection models. The results suggest that PC2 may play an important role in the development of BBB instability and that PC1-to-PC2 transition may be a physiologically more relevant phenomenon during BBB breakdown to study than pericyte loss.

Acknowledgements

We thank the NIH NeuroBioBank (https://neurobiobank.nih.gov) for graciously providing postmortem human brain tissues. The NIH NeuroBioBank is supported by the National Institute of Mental Health (NIMH).

This work was supported by NIH Grants R01MH107333 (W.-K.K.) and R21MH108458 (W.-K.K.); also supported in part by R01AI097059 (M.J.K.), R33AI110163 (M.J.K), and R56AG052349 (E.S.D.).

Bibliography

Alarcon-Martinez L, Yilmaz-Ozcan S, Yemisci M, Schallek J, Kilic K, Can A, Di Polo A, Dalkara T, 2018 Capillary pericytes express alpha-smooth muscle actin, which requires prevention of filamentous-actin depolymerization for detection. Elife 7.

Armulik A, Genove G, Mae M, Nisancioglu MH, Wallgard E, Niaudet C, He L, Norlin J, Lindblom P, Strittmatter K, Johansson BR, Betsholtz C, 2010 Pericytes regulate the blood-brain barrier. Nature 468(7323), 557–561. [PubMed: 20944627]

Attwell D, Mishra A, Hall CN, O'Farrell FM, Dalkara T, 2016 What is a pericyte? J. Cereb. Blood Flow Metab 36(2), 451–455. [PubMed: 26661200]

Balabanov R, Dore-Duffy P, 1998 Role of the CNS microvascular pericyte in the blood-brain barrier. J. Neurosci. Res 53(6), 637–644. [PubMed: 9753191]

Bhagwat SV, Lahdenranta J, Giordano R, Arap W, Pasqualini R, Shapiro LH, 2001 CD13/APN is activated by angiogenic signals and is essential for capillary tube formation. Blood 97(3), 652–659. [PubMed: 11157481]

Boado RJ, Pardridge WM, 1994 Differential expression of alpha-actin mRNA and immunoreactive protein in brain microvascular pericytes and smooth muscle cells. J. Neurosci. Res 39(4), 430–435. [PubMed: 7884822]

Bohannon DG, Ko A, Filipowicz AR, Kuroda MJ, Kim WK, 2019 Dysregulation of sonic hedgehog pathway and pericytes in the brain after lentiviral infection. J. Neuroinflammation 16(1), 86. [PubMed: 30981282]

Castejon OJ, 2011 Ultrastructural pathology of cortical capillary pericytes in human traumatic brain oedema. Folia Neuropathol 49(3), 162–173. [PubMed: 22101949]

Chasseigneaux S, Moraca Y, Cochois-Guegan V, Boulay AC, Gilbert A, Le Crom S, Blugeon C, Firmo C, Cisternino S, Laplanche JL, Curis E, Decleves X, Saubamea B, 2018 Isolation and differential transcriptome of vascular smooth muscle cells and mid-capillary pericytes from the rat brain. Sci. Rep 8(1), 12272. [PubMed: 30116021]

Costa MA, Paiva AE, Andreotti JP, Cardoso MV, Cardoso CD, Mintz A, Birbrair A, 2018 Pericytes constrict blood vessels after myocardial ischemia. J Mol Cell Cardiol 116, 1–4. [PubMed: 29371134]

Crisan M, Chen CW, Corselli M, Andriolo G, Lazzari L, Peault B, 2009 Perivascular multipotent progenitor cells in human organs. Ann. N. Y. Acad. Sci 1176, 118–123. [PubMed: 19796239]

Dore-Duffy P, Cleary K, 2011 Morphology and properties of pericytes. Methods Mol. Biol 686, 49–68. [PubMed: 21082366]

Farrall AJ, Wardlaw JM, 2009 Blood-brain barrier: ageing and microvascular disease--systematic review and meta-analysis. Neurobiol. Aging 30(3), 337–352. [PubMed: 17869382]

Fernandez-Klett F, Priller J, 2015 Diverse functions of pericytes in cerebral blood flow regulation and ischemia. J Cereb Blood Flow Metab 35(6), 883–887. [PubMed: 25853910]

Fuller RA, Westmoreland SV, Ratai E, Greco JB, Kim JP, Lentz MR, He J, Sehgal PK, Masliah E, Halpern E, Lackner AA, Gonzalez RG, 2004 A prospective longitudinal in vivo 1H MR spectroscopy study of the SIV/macaque model of neuroAIDS. BMC. Neurosci 5, 10.

Grant RI, Hartmann DA, Underly RG, Berthiaume AA, Bhat NR, Shih AY, 2019 Organizational hierarchy and structural diversity of microvascular pericytes in adult mouse cortex. J. Cereb. Blood Flow Metab 39(3), 411–425. [PubMed: 28933255]

Guillemin GJ, Brew BJ, 2004 Microglia, macrophages, perivascular macrophages, and pericytes: a review of function and identification. J. Leukoc. Biol 75(3), 388–397. [PubMed: 14612429]

Hartmann DA, Underly RG, Grant RI, Watson AN, Lindner V, Shih AY, 2015 Pericyte structure and distribution in the cerebral cortex revealed by high-resolution imaging of transgenic mice. Neurophotonics 2(4), 041402.

Herman IM, D'Amore PA, 1985 Microvascular pericytes contain muscle and nonmuscle actins. J. Cell Biol 101(1), 43–52. [PubMed: 3891763]

Jeon H, Ono M, Kumagai C, Miki K, Morita A, Kitagawa Y, 1996 Pericytes from microvessel fragment produce type IV collagen and multiple laminin isoforms. Biosci. Biotechnol. Biochem 60(5), 856–861. [PubMed: 8704315]

Krueger M, Bechmann I, 2010 CNS pericytes: concepts, misconceptions, and a way out. Glia 58(1), 1–10. [PubMed: 19533601]

Kumar A, D'Souza SS, Moskvin OV, Toh H, Wang B, Zhang J, Swanson S, Guo LW, Thomson JA, Slukvin II, 2017 Specification and Diversification of Pericytes and Smooth Muscle Cells from Mesenchymoangioblasts. Cell Rep 19(9), 1902–1916. [PubMed: 28564607]

Lauridsen HM, Pellowe AS, Ramanathan A, Liu R, Miller-Jensen K, McNiff JM, Pober JS, Gonzalez AL, 2017 Tumor Necrosis Factor-alpha and IL-17A Activation Induces Pericyte-Mediated Basement Membrane Remodeling in Human Neutrophilic Dermatoses. Am. J. Pathol 187(8), 1893–1906. [PubMed: 28609645]

Montagne A, Barnes SR, Sweeney MD, Halliday MR, Sagare AP, Zhao Z, Toga AW, Jacobs RE, Liu CY, Amezcua L, Harrington MG, Chui HC, Law M, Zlokovic BV, 2015 Blood-brain barrier breakdown in the aging human hippocampus. Neuron 85(2), 296–302. [PubMed: 25611508]

Nakazato R, Kawabe K, Yamada D, Ikeno S, Mieda M, Shimba S, Hinoi E, Yoneda Y, Takarada T, 2017 Disruption of Bmal1 Impairs Blood-Brain Barrier Integrity via Pericyte Dysfunction. J. Neurosci 37(42), 10052–10062. [PubMed: 28912161]

Persidsky Y, Ramirez SH, Haorah J, Kanmogne GD, 2006 Blood-brain barrier: structural components and function under physiologic and pathologic conditions. J. Neuroimmune. Pharmacol 1(3), 223–236. [PubMed: 18040800]

Peters A, Sethares C, 2012 Age-related changes in the morphology of cerebral capillaries do not correlate with cognitive decline. J. Comp Neurol 520(6), 1339–1347. [PubMed: 22102171]

Podjaski C, Alvarez JI, Bourbonniere L, Larouche S, Terouz S, Bin JM, Lecuyer MA, Saint-Laurent O, Larochelle C, Darlington PJ, Arbour N, Antel JP, Kennedy TE, Prat A, 2015 Netrin 1 regulates blood-brain barrier function and neuroinflammation. Brain 138(Pt 6), 1598–1612. [PubMed: 25903786]

Sengillo JD, Winkler EA, Walker CT, Sullivan JS, Johnson M, Zlokovic BV, 2013 Deficiency in mural vascular cells coincides with blood-brain barrier disruption in Alzheimer's disease. Brain Pathol 23(3), 303–310. [PubMed: 23126372]

Skalli O, Pelte MF, Peclet MC, Gabbiani G, Gugliotta P, Bussolati G, Ravazzola M, Orci L, 1989 Alpha-smooth muscle actin, a differentiation marker of smooth muscle cells, is present in microfilamentous bundles of pericytes. J. Histochem. Cytochem 37(3), 315–321. [PubMed: 2918221]

Stratman AN, Schwindt AE, Malotte KM, Davis GE, 2010 Endothelial-derived PDGF-BB and HB-EGF coordinately regulate pericyte recruitment during vasculogenic tube assembly and stabilization. Blood 116(22), 4720–4730. [PubMed: 20739660]

Sweeney MD, Ayyadurai S, Zlokovic BV, 2016 Pericytes of the neurovascular unit: key functions and signaling pathways. Nat. Neurosci 19(6), 771–783. [PubMed: 27227366]

Verbeek MM, Otte-Holler I, Wesseling P, Ruiter DJ, de Waal RM, 1994 Induction of alpha-smooth muscle actin expression in cultured human brain pericytes by transforming growth factor-beta 1. Am. J. Pathol 144(2), 372–382. [PubMed: 8311120]

Villasenor R, Kuennecke B, Ozmen L, Ammann M, Kugler C, Gruninger F, Loetscher H, Freskgard PO, Collin L, 2017 Region-specific permeability of the blood-brain barrier upon pericyte loss. J. Cereb. Blood Flow Metab 37(12), 3683–3694. [PubMed: 28273726]

Wang S, Cao C, Chen Z, Bankaitis V, Tzima E, Sheibani N, Burridge K, 2012 Pericytes regulate vascular basement membrane remodeling and govern neutrophil extravasation during inflammation. PLoS. ONE 7(9), e45499.

Zhao Z, Nelson AR, Betsholtz C, Zlokovic BV, 2015 Establishment and Dysfunction of the Blood-Brain Barrier. Cell 163(5), 1064–1078. [PubMed: 26590417]

Highlights:

- Identified a distinct subset of pericytes, PC2, which are found on CNS microvessels.
- The proportion of PC2 increases with age and SIV infection status.
- PC2 are associated with disrupted BBB and decreased expression of claudin-5.

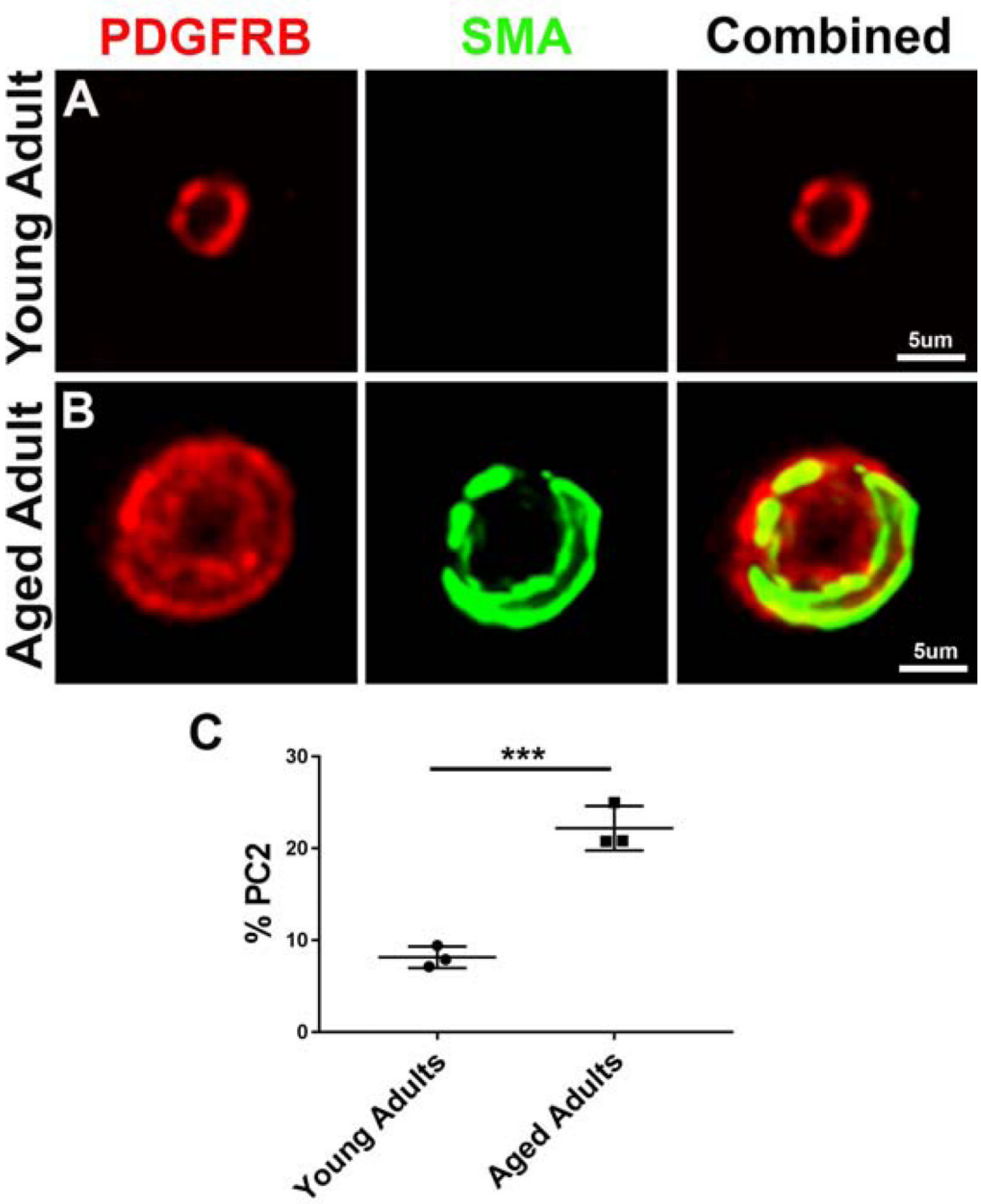

Figure 1. Distinct secondary pericyte morphology increasingly present in aging human prefrontal cortex

Double IF for PDGFRB (red) and SMA (green) reveals two distinct pericyte morphologies in both young adult (a) and aged adult (b) human brain sections. Aged adults had significantly more PDGFRB+/SMA+ pericyte-associated vessels than young adults (c). Error bars denote standard deviation. An un-paired t-test was performed (c).

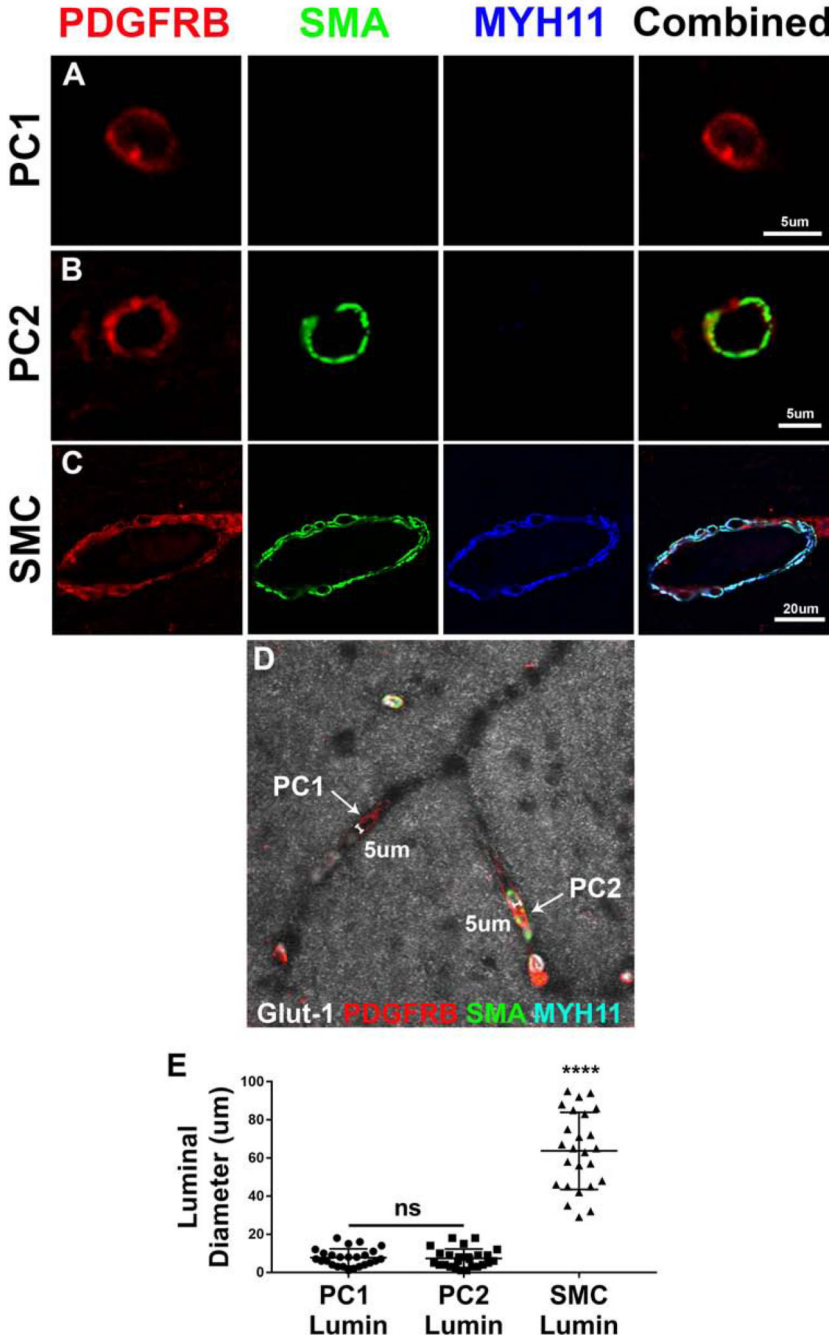

Figure 2. Phenotyping of pericyte and smooth muscle cell populations in the brain of uninfected young adult rhesus macaques

Triple immunofluorescent imaging of PC1, PC2, and SMCs for PDGFRB (red), SMA (green) and MYH11 (blue) distinguishes three distinct phenotypes between the three populations (a-c). PC1s are PDGFRB+ SMA− and MYH11− (a) while PC2 are PDGFRB+ SMA+ and MYH11− (b). Only SMCs are positive for all three markers (c). A four-color IF image, with an overlay of differential interference contrast image (grey), for GLUT1 (white), PDGFRB (red), SMA (green), and MYH11 (cyan) shows a branching microvessel with a PC1 on one arm or the branch and a PC2 on the other and no MYH11+ SMCs present on

either arm. PC1− and PC2-associated vessel branches are 5 um in luminal diameter and equivalent in branching order and size (d). Vascular luminal diameter associated with PC1 and PC2s showed no significant difference, while vessels with SMC coverage are significantly larger in luminal diameter (e). Error bars denote standard deviation. A one-way ANOVA was performed (e).

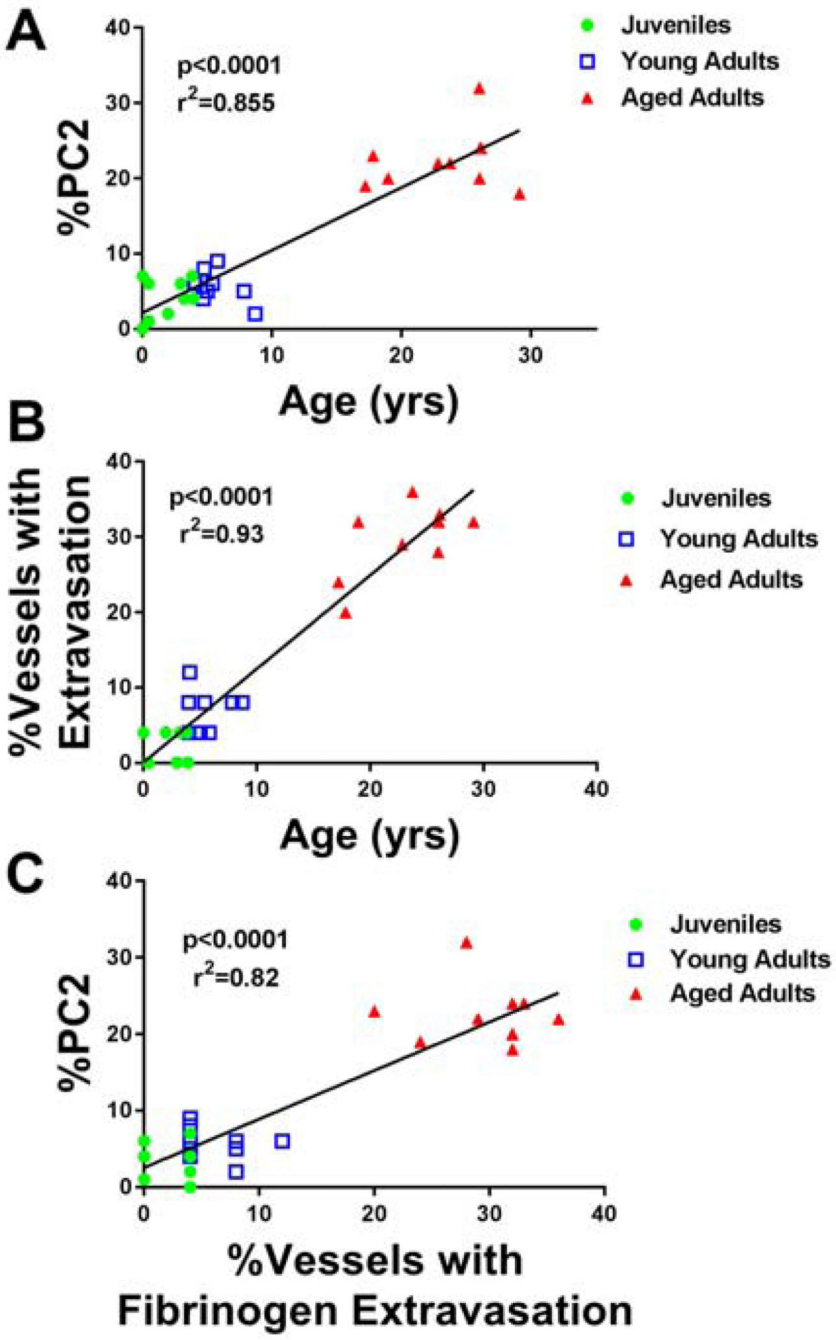

Figure 3. Percentage of PC2 and fibrinogen extravasation increase with age

The percentage of measured pericytes which were PC2 is significantly positively correlated to the age of the animal (a). The percentage of measured vessels demonstrating fibrinogen extravasation is significantly positively correlated to the age of the animal (b). A significant positive correlation exists between the percent of vessels with PC2 coverage and the percent of vessels with fibrinogen extravasation in each animal measured (c). All points on the graphs depict one animal (a-c). Linear regressions were performed between all three groups (a-c).

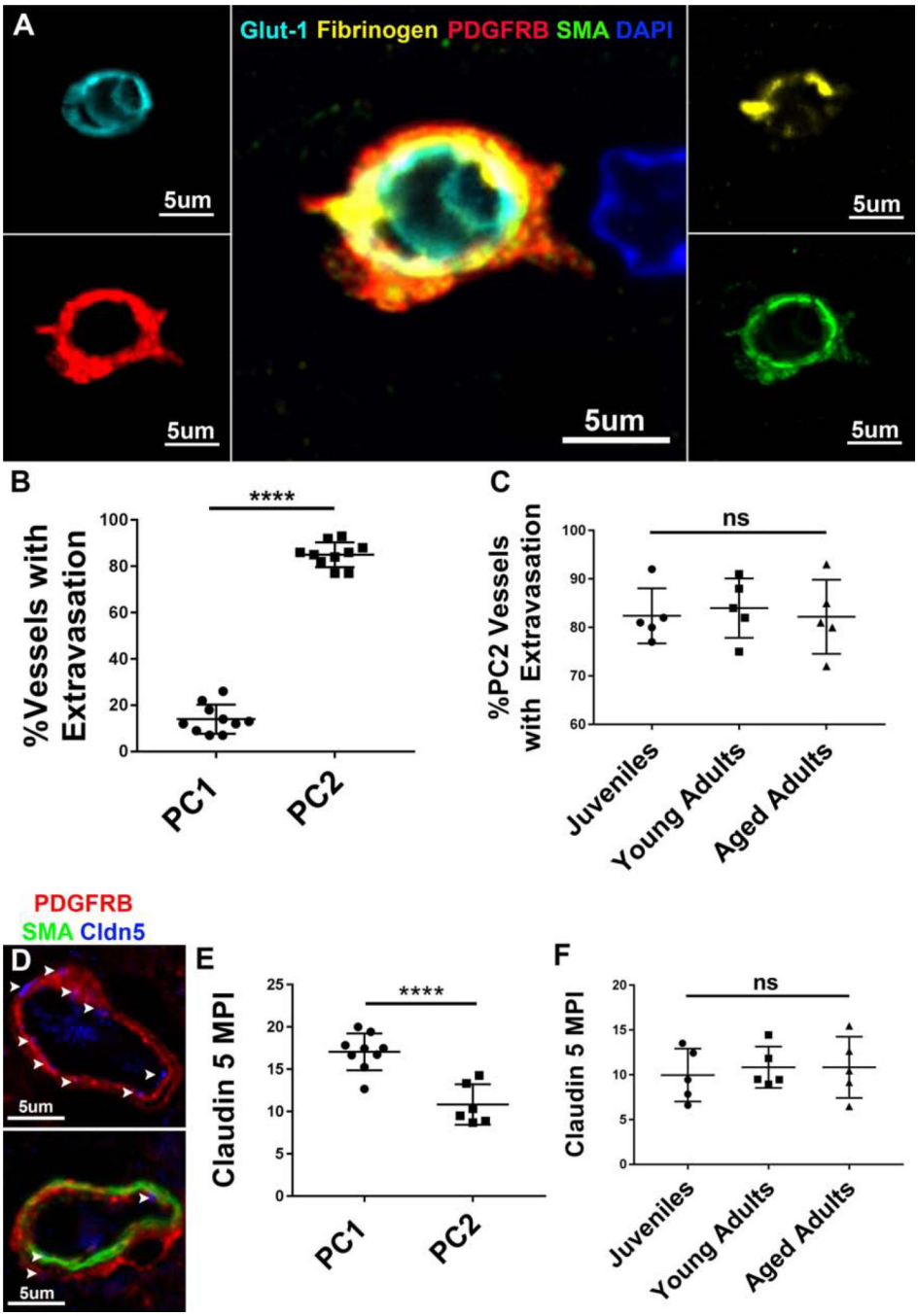

Figure 4. PC2 show reduced BBB angiogenic function independent of age

A representative five color IF image of a PC2 vessels in an aged rhesus macaque shows endothelial cells with GLUT1 (cyan), pericytes with PDGFRB (red) and SMA (green), fibrinogen (yellow), and nuclei with DAPI (dark blue) demonstrating fibrinogen leaking from a discontinuous endothelial layer and spilling out into the PC2 layer (a). Vessels with PC2 coverage were found to be significantly more likely to have fibrinogen extravasation than vessels with PC1 coverage via triple immunofluorescence dual overlay histograms (b). There was no significant difference in the instance of fibrinogen extravasation in PC2

vessels according to age group (c). Triple immunofluorescence microscopy images of PC1 (top) and PC2 (bottom) vessels with PDGFRB (red) SMA (green) and claudin 5 (blue) demonstrating differential levels of claudin 5 expression (d). Vessels with PC2 coverage were found to have significantly lower levels of claudin 5 immunoreactivity when compared to PC1 associated vessels (e). MPI of claudin 5 for PC2 vessels did not change significantly between age groups (f). Arrowheads denote claudin 5 positive areas on pericytes (d). Error bars denote standard deviation. An unpaired t-test was performed (b,e) and a one-way ANOVA was performed (c,f).

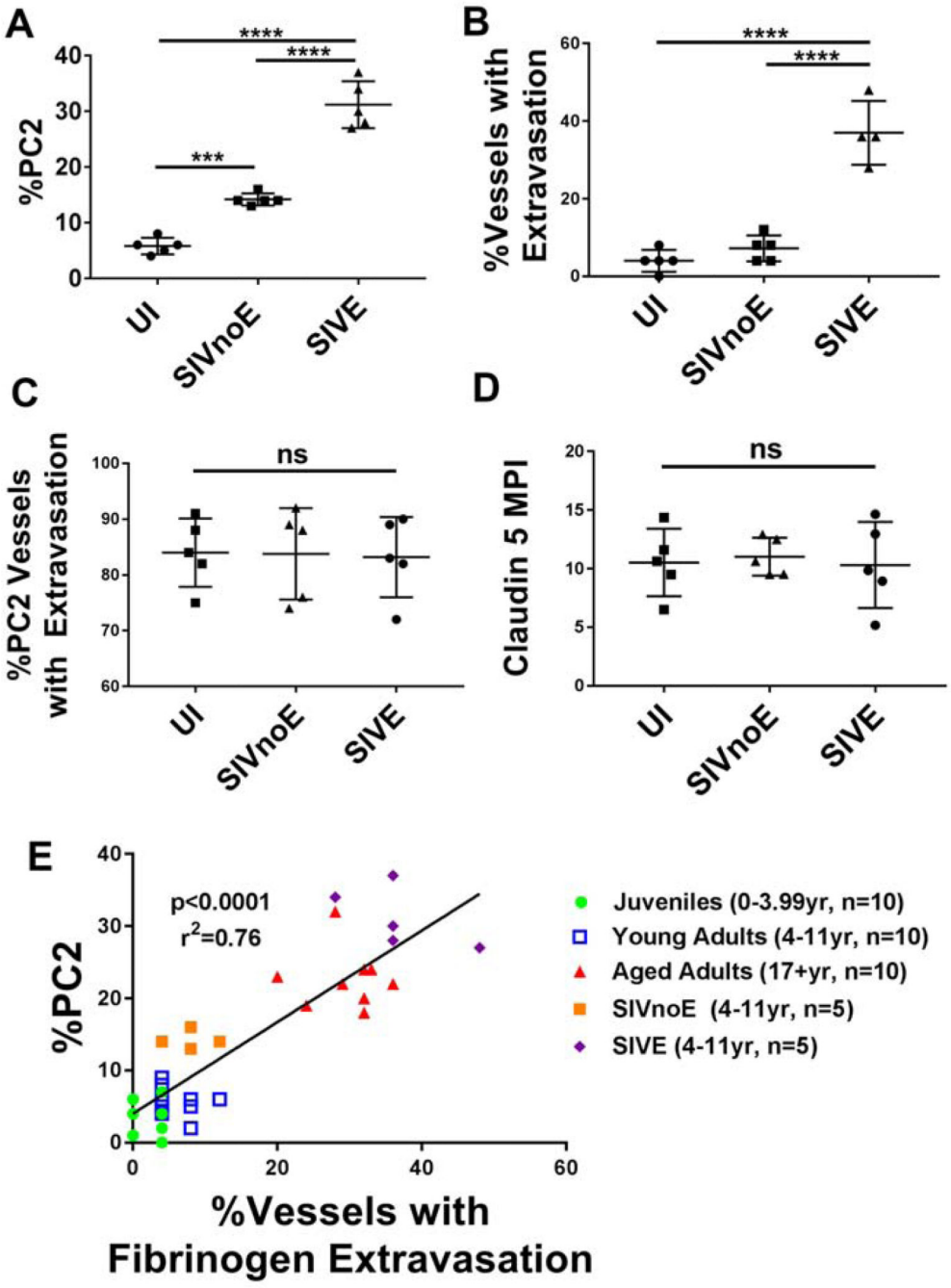

Figure 5. Percentage of PC2s and fibrinogen extravasation increase with SIV infection

The percentage of measured pericytes which were SMA+ PC2 is significantly higher in SIVnoE and SIVE animals than their age and gender matched uninfected counterparts (a). The percentage of measured vessels demonstrating fibrinogen extravasation is significantly higher in SIVE animals than uninfected age- and gender-matched counterparts (b). There was no significant difference in the instance of fibrinogen extravasation or MPI of claudin 5 in PC2 vessels according to disease status (c-d). There is a significant positive correlation between the % of vessels with fibrinogen extravasation and the % of pericytes which are

PC2 independent of age or disease status when all groups are combined (e). Each point on the graph depicts one animal (e). Error bars denote standard deviation. A one-way ANOVA was performed (a-d) and a linear regression was performed between all 5 groups (e).

Table 1.

Human materials used in study (a). Animals used in study (b).

A.			
Human ID	**Group**	**Age**	**Gender**
HCT17HEO	Young Uninfected Adult	34	Male
HCT15HAW	Young Uninfected Adult	22	Male
HCT17HEV	Young Uninfected Adult	30	Female
HCTZA	Aged Uninfected Adult	79	Female
01965	Aged Uninfected Adult	63	Female
01640	Aged Uninfected Adult	63	Male
B.			
Macaque ID	**Group**	**Age**	**Gender**
12A448	Uninfected Juvenile	0.36	F
12A447	Uninfected Juvenile	0.37	F
16A499	Uninfected Juvenile	0.45	M
15A524	Uninfected Juvenile	0.5	F
12A006	Uninfected Juvenile	0.52	F
15A313	Uninfected Juvenile	1.99	M
15A312	Uninfected Juvenile	2.96	M
14A342	Uninfected Juvenile	3.23	F
16A059	Uninfected Juvenile	3.86	M
14A311	Uninfected Juvenile	3.95	M
14A351	Young Uninfected Adult	4.02	F
14A325	Young Uninfected Adult	4.09	F
11A023	Young Uninfected Adult	4.69	M
11A014	Young Uninfected Adult	4.77	M
11A313	Young Uninfected Adult	5.02	M
11A635	Young Uninfected Adult	5.41	M
16A062	Young Uninfected Adult	5.81	F
18A087	Young Uninfected Adult	7.86	M
18A039	Young Uninfected Adult	8.73	M
11A314	Young Uninfected Adult	8.99	M
17A517	Aged Uninfected Adult	17.21	F
17A029	Aged Uninfected Adult	17.83	M
17A397	Aged Uninfected Adult	18.97	F
16A070	Aged Uninfected Adult	22.83	F
17A059	Aged Uninfected Adult	23.75	F
#352	Aged Uninfected Adult	26	M
17A195	Aged Uninfected Adult	26.03	F
17A193	Aged Uninfected Adult	26.07	F

A.			
Human ID	**Group**	**Age**	**Gender**
17A196	Aged Uninfected Adult	26.15	F
17A424	Aged Uninfected Adult	29.12	M
10A067	SIV with Encephalitis	5.7	M
11A554	SIV with Encephalitis	10.28	M
11A562	SIV with Encephalitis	5.15	M
13A400	SIV with Encephalitis	5.96	M
10A786	SIV with Encephalitis	10.68	M
11A023	SIV without Encephalitis	4.69	M
11A014	SIV without Encephalitis	4.77	M
11A313	SIV without Encephalitis	5.02	M
11A635	SIV without Encephalitis	5.41	M
11A314	SIV without Encephalitis	8.99	M

Table 2.

Antibodies used in this study.

Antibody	Clone	Ig Type	Manufacturer	Catalog	Dilution
Claudin 5	N/A	Rabbit IgG	Springer	E3754	1:250
Fibrinogen	N/A	Rabbit IgG	Abcam	Ab58207	1:100
GLUT1	SPM498	Mouse IgG2a	Thermo	MA1-37783	1:200
MYH11	N/A	Rabbit IgG	Sigma	HPA015310	1:30
PDGFRB	Y92	Rabbit IgG	Abcam	ab32570	1:20
PDGFRB	Y92	Rabbit IgG AF594 Pre-Conjugated	Abcam	ab206872	1:10
SMA	D4K9N	Rabbit IgG AF488 Pre-Conjugated	Cell Signaling	34105S	1:100
AF594	N/A	Multiple	Thermo	Multiple	1:500
AF488	N/A	Multiple	Thermo	Multiple	1:500
BV480	N/A	Goat anti-Rabbit H+L	Jackson Immuno	111658144	1:200
CF350	N/A	Goat anti-Mouse IgG1	Biotium	20245	1:500